Plant Physiol. (1997) 115: 593–598

Molecular Rigidity in Dry and Hydrated Onion Cell Walls[1]

Marie-Ann Ha, David C. Apperley, and Michael C. Jarvis*

Chemistry Department, Glasgow University, Glasgow G12 8QQ, Scotland, United Kingdom (M.-A.H., M.C.J.); and Engineering and Physical Sciences Research Council Solid-State Nuclear Magnetic Resonance Service, Durham University, Durham DH1 3LE, United Kingdom (D.C.A.)

Solid-state nuclear magnetic resonance relaxation experiments can provide information on the rigidity of individual molecules within a complex structure such as a cell wall, and thus show how each polymer can potentially contribute to the rigidity of the whole structure. We measured the proton magnetic relaxation parameters T_2 (spin-spin) and $T_{1\rho}$ (spin-lattice) through the ^{13}C-nuclear magnetic resonance spectra of dry and hydrated cell walls from onion (*Allium cepa* L.) bulbs. Dry cell walls behaved as rigid solids. The form of their T_2 decay curves varied on a continuum between Gaussian, as in crystalline solids, and exponential, as in more mobile materials. The degree of molecular mobility that could be inferred from the T_2 and $T_{1\rho}$ decay patterns was consistent with a crystalline state for cellulose and a glassy state for dry pectins. The theory of composite materials may be applied to explain the rigidity of dry onion cell walls in terms of their components. Hydration made little difference to the rigidity of cellulose and most of the xyloglucan shared this rigidity, but the pectic fraction became much more mobile. Therefore, the cellulose/xyloglucan microfibrils behaved as solid rods, and the most significant physical distinction within the hydrated cell wall was between the microfibrils and the predominantly pectic matrix. A minor xyloglucan fraction was much more mobile than the microfibrils and probably corresponded to cross-links between them. Away from the microfibrils, pectins expanded upon hydration into a nonhomogeneous, but much softer, almost-liquid gel. These data are consistent with a model for the stress-bearing hydrated cell wall in which pectins provide limited stiffness across the thickness of the wall, whereas the cross-linked microfibril network provides much greater rigidity in other directions.

Little is known about the details of how the structure of plant cell walls gives them their rigidity and strength, and thus their ability to support the plant against the stresses of weather, gravity, and transpiration (Raven, 1977; Preston, 1979). Solid-state NMR spectrometry has the potential to provide a window into the internal stress-bearing properties of the cell wall. Magnetic relaxation data derived from NMR experiments allow the relative mobilities of individual polymers, and of functional groups within them, to be inferred (Abragam, 1961).

Much of the relevant NMR methodology, and the theory for linking polymer mobility to bulk mechanical properties, have been developed for synthetic macromolecules (Schaefer et al., 1977; Kenwright and Say, 1993; McBrierty and Packer, 1994). Similar experiments have been carried out on plant cell walls (Irwin et al., 1984, 1985; Newman et al., 1994, 1996; Foster et al., 1996; Ha et al., 1996), but the full transfer of the technology from synthetic polymers to hydrated biological materials such as the cell wall is not likely to be simple. It will require solutions to substantial experimental problems arising from the presence of water, and a detailed understanding of the architecture of the cell wall at the molecular and supramolecular scale, so that the distribution of internal stresses in response to any external stress can be predicted.

In this paper we take some preliminary steps toward this goal by describing proton magnetic relaxation rates in onion (*Allium cepa* L.) cell walls, for which detailed architectural information is available from the electron microscopy work of McCann et al. (1990, 1992). Their polysaccharide composition is well established: the major components are cellulose, galactan-rich pectins, and xyloglucans (Mankarios et al., 1979; Ishii, 1982; Redgwell and Selvendran, 1986; Ryden et al., 1989). The onion cell walls were studied both dry and hydrated, because it is well known that removal of water from such materials drastically alters their macroscopic mechanical properties.

MATERIALS AND METHODS

Cell Walls

Chopped bulb tissue from onion (*Allium cepa* L. cv Bobosa) (100 g) was homogenized in 500 mL of Triton X-100 (2 g L^{-1}), and cell walls were collected on a sintered glass funnel. The walls were washed with water and the excess liquid was removed by suction. The walls were then stirred for 30 min in 15 mL of phenol-saturated water, washed extensively with water, cryomilled in liquid N_2, and dried to a 2.4:1 wall to water ratio prior to NMR.

NMR Methods

Measurements of proton relaxation behavior were derived through the ^{13}C spectra in CP-MAS experiments, using a spectrometer (model VXR-300, Varian, San Fernando, CA) fitted with Teflon seals on the rotor end-caps to retain water. The proton field applied was approximately

[1] This work was financially supported by the Biotechnology and Biological Science Research Council and the Engineering and Physical Sciences Research Council.

* Corresponding author; e-mail mikej@chem.gla.ac.uk; fax 44–141–330–4888.

Abbreviations: CP, cross-polarization; MAS, magic-angle spinning; $T_{1\rho}$, spin-lattice relaxation time constant; T_2, spin-spin relaxation time constant.

60 kHz during both CP and data acquisition. The Hartmann-Hahn matching condition was adjusted individually for each sample by reducing the ^{13}C field until signal intensity was optimized. The magnitude of the adjustment required for the hydrated sample implied significant absorption of proton radio-frequency energy by water. A recycle time of 1 s allowed essentially complete laboratory-frame spin-lattice relaxation of protons between scans. Resonance assignments are based on published data (Jarvis, 1990; Newman et al., 1994; Ha et al., 1996). The assignment of the 82.5-ppm chemical shift to C-4 of the glucan chain of xyloglucan is derived from proton spin-diffusion experiments (M.A. Ha and M.C. Jarvis, unpublished data) showing that the polymer giving rise to this resonance is distinct from cellulose and from pectins, and is located outside cellulose at the surface of the microfibrils.

The proton T_2 was measured in a CP-MAS experiment modified by the insertion of a variable delay (T_s) between the initial proton 90° pulse and the contact pulse (Tekely and Vignon, 1987; Newman, 1992). Since proton T_2 relaxation can be modeled as either Gaussian, for crystalline solids, or exponential, for more mobile materials, the decay of the signal intensity with T_s was fitted to the following equation:

$$S = S_0 \exp - (T_s/T_2)^n \quad (1)$$

where S is the signal intensity, S_0 is the signal intensity at $T_s = 0$, and $1 < n < 2$.

Gaussian behavior corresponds to $n = 2$ and exponential behavior to $n = 1$. This procedure allowed for relaxation curves intermediate between these two extremes (Kenwright and Say, 1993). An alternative model expresses the total signal intensity S as the sum of a Gaussian and an exponential component, so that:

$$S = S_1 \exp - (T_s/T_2) + (S_0 - S_1) \exp - (T_s/T_2)^2 \quad (2)$$

where S_1 is the intensity of the exponential component of the signal.

Whenever the signal to noise ratio was sufficient to distinguish between these two models, the model expressed by Equation 1 gave a closer fit to the data, and this model was therefore used throughout.

The rotating-frame proton $T_{1\rho}$ was determined in a standard delayed-contact experiment and modeled by least-squares fitting as either a one- or a two-component exponential.

RESULTS

^{13}C Spectra

The ^{13}C spectra of dry and hydrated onion cell walls are shown in Figure 1. The spectral resolution was lower for the dry sample, a normal observation with cell walls because of conformational variation, which causes a spread in chemical shift for each resonance. This conformational spread is reduced in hydrated samples by motional averaging (Jarvis et al., 1996).

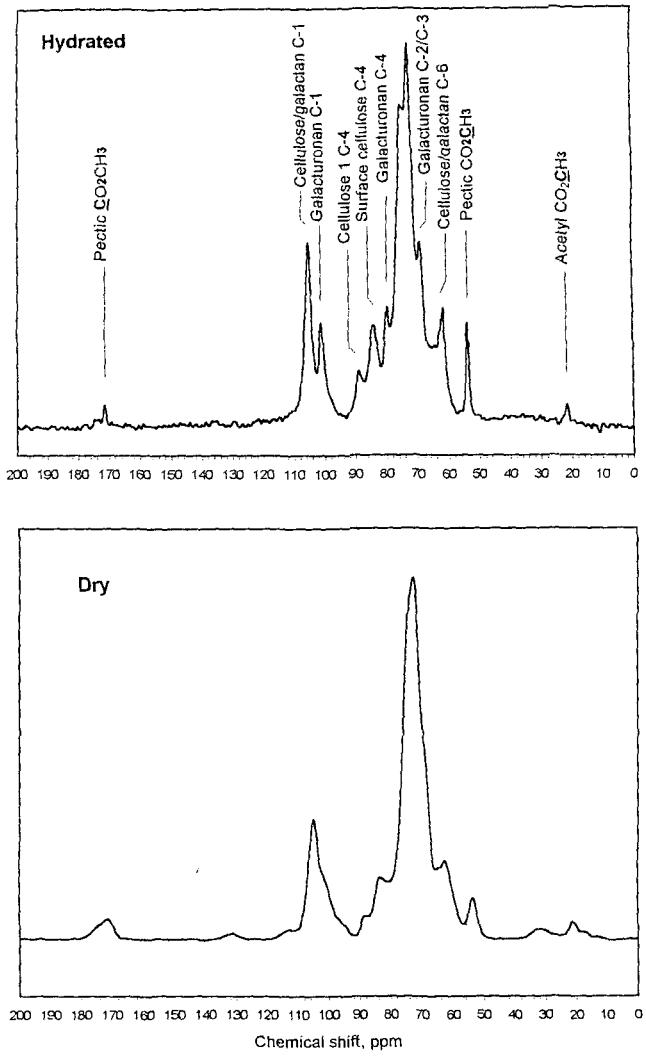

Figure 1. ^{13}C CP-MAS NMR spectra of dry and hydrated onion cell walls. The hydrated cell walls had water added in the ratio 2.4:1.

Relaxation Measurements on Dry Cell Walls

Proton T_2 Measurements

Proton T_2 values increase with thermal motion on the kilohertz frequency scale, and range from 8 to 9 μs for rigid crystalline solids to milliseconds for liquids (Newman 1992; Ha et al., 1996). Dry onion cell walls showed a narrow range of T_2 values close to the crystalline limit (Fig. 2). The T_2 for methyl ester groups was slightly elevated, but this may be assumed to be due to methyl rotation rather than motions of the entire polymer chain (Jarvis et al., 1996). The dry cell walls, therefore, were too rigid for the proton T_2 to be a very sensitive indicator of molecular flexibility.

The form of the T_2 decay curve also can be informative about motions within a solid. In theory, for a highly crystalline solid the decay is Gaussian, whereas for liquids it is exponential. A detailed theoretical description is not available for intermediate forms of decay, but the decay curves observed here (Fig. 2) clearly lay between the Gaussian and

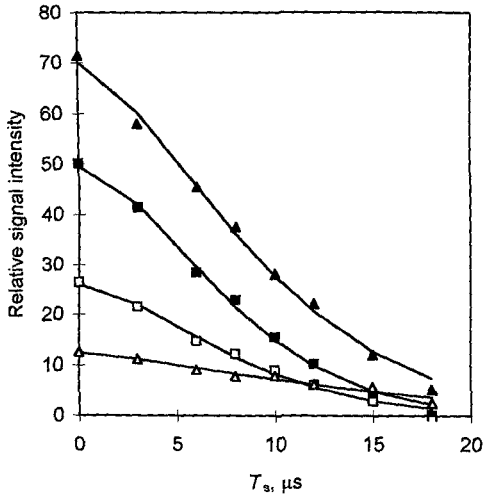

Figure 2. Proton T_2 relaxation curves for principal peaks in the ^{13}C-NMR spectrum of dry onion cell walls. Rapid relaxation (short T_2) implies low molecular mobility. Peak assignments are as follows: ■, 105 ppm, C-1 of cellulose and galactan, n = 1.7, T_2 = 9.0 μs; □, 84 ppm, C-4 of crystal-surface cellulose, n = 1.6, T_2 = 9.1 μs; ▲, 69 ppm, C-2 and C-3 of galacturonan, n = 1.5, T_2 = 10.5 μs; and △, 54 ppm, galacturonan methyl ester, n = 1.4, T_2 = 15.4 μs. Peak intensity is plotted against T_s, the time allowed for spin-spin relaxation of proton magnetization before the magnetization is passed to ^{13}C by cross-polarization. Fitted curves were derived from Equation 1 (see "Materials and Methods") using values of the exponent n between the Gaussian limit of 2.0 and the exponential limit of 1.0.

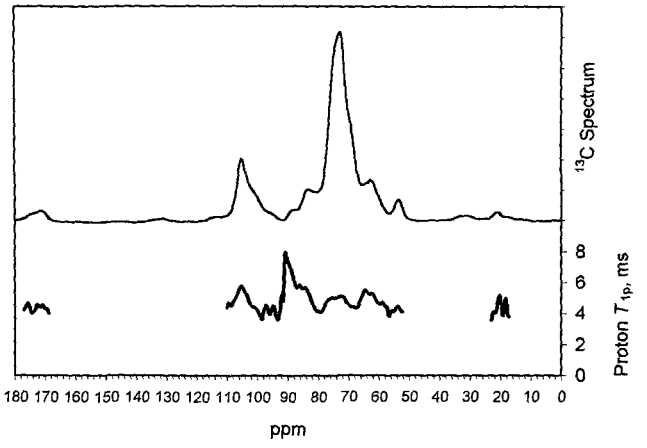

Figure 3. Proton rotating-frame $T_{1\rho}$ plotted across the ^{13}C-NMR spectrum of dry onion cell walls. Rapid relaxation (short $T_{1\rho}$) implies high molecular mobility. Gaps in the plot correspond to spectral regions with near-baseline intensity where the T_2 could not be calculated. See Figure 1 for peak assignments.

exponential extremes ($1 < n < 2$), and the exponent n appeared to be a useful indicator of molecular motion in addition to the T_2 itself. It is possible that the observed values of n and T_2 are partially averaged between pectins and crystalline cellulose by proton spin diffusion, and that without this effect n would have been closer to the limits of 1 and 2, respectively, for the pectic and cellulosic components.

Proton $T_{1\rho}$ Measurements

In plant cell walls proton $T_{1\rho}$ values normally decrease with thermal motion on the 10^3- to 10^4-Hz frequency scale (Jarvis et al., 1996; Newman et al., 1996). Spin diffusion averages the proton $T_{1\rho}$ across adjacent polymer molecules to a much greater extent than the proton T_2 because it can occur for 10 ms or more during the measurement of the $T_{1\rho}$ but only for about 1 ms (the contact time) during the T_2 measurement. Proton spin diffusion is most efficient in crystalline solids, in which immobile protons are in close proximity to one another. In more mobile systems its efficiency decreases with increasing proton T_2 (Newman, 1992).

Proton spin diffusion has also been used to elucidate spatial relationships between pectins and other components of cell walls (Ha et al., 1996). In dry onion cell walls the proton $T_{1\rho}$ showed little variation around a mean of 5 ms (Fig. 3), because averaging by spin diffusion was clearly efficient, as would be expected from the proton T_2 values. However, the $T_{1\rho}$ values for the pectic resonances (171, 101, 80, 69, and 54 ppm) were consistently shorter than the rest, and the longest value recorded was for C-4 of cellulose I (89 ppm) at the core of the cellulose crystalline regions, which was the farthest away from the influence of the more mobile pectins. The principal relaxation route is likely to have been through rotating pectic methyl groups (Jarvis et al., 1996), so that the $T_{1\rho}$ increased with the mean distance from these.

Taking the proton $T_{1\rho}$, T_2, and n together, the proton relaxation data were consistent with a crystalline state for cellulose in the dry cell walls. The pectic polysaccharides do not readily form crystalline solids, although restricted domains within them (junction zones in the gel state, and domains derived from these in the dry solid) do show short-range order (Jarvis and Apperley, 1995, and refs. therein). Since the proton relaxation data indicated a de-

Table I. *Proton spin-spin relaxation parameters for hydrated onion cell walls, fitted to a two-component model with component 1 (n = 1.5) corresponding to the microfibril fraction and component 2 (n = 1.0) corresponding to the pectic matrix*

Resonance[a]	Component 1	T_2(1)	T_2(2)
	%	μs	
Galacturonan C-6 (171)	0	–	31
Cellulose/galactan C-1 (105)	83	11.4	>100
Galacturonan C-1 (101)	0	–	41
Cellulose I C-4 (89)	100	11.8	–
Cellulose C-4 (84)	96	10.9	40
Xyloglucan C-4 (82.5)	55	10.6	40
Galacturonan C-4 (80)	28	12.3	48
Galacturonan C-2/3 (69)	6	12.0	43
Cellulose I C-6 (65)	100	11.9	–
Cellulose/galactan C-6 (62)	60	9.3	>100
Pectin methoxyl (54)	0	–[b]	>100
Acetyl (21)	0	–[b]	81

[a] Numbers in parentheses indicate ^{13}C chemical shift in ppm.

gree of rigidity close to that of cellulose, it seems reasonable to describe the pectic matrix as a glassy solid.

Relaxation Measurements on Hydrated Cell Walls

Proton T_2 Measurements

Hydration left the proton T_2 for the cellulosic resonances almost unchanged (Table I), but proton T_2 values for pectins were much longer than in the dry cell walls and some of the decay curves did not fit Equation 1 closely unless it was assumed that more than one component was present. The decay curves for cellulose (65, 84, and 89 ppm) could be fitted closely by a function with $n = 1.5$, intermediate between the Gaussian and exponential limits (data not shown). Since the number of variables that can be handled simultaneously by least-squares fitting is limited by the signal to noise ratio of the spectra, the decay curves were modeled as the sum of two functions with $n = 1.5$ and $n = 1.0$, respectively, corresponding to the microfibril and matrix phases. This is a minimal interpretation, because it may be assumed that two or more pectic components were present in the matrix.

Table I shows that the cell wall polymers can be divided into three groups on the basis of their spin-spin relaxation kinetics. One group, with a T_2 of approximately 11 ms, includes cellulose, the majority of the xyloglucan, and a small proportion of the galacturonan chains. The second group, with a T_2 of approximately 40 ms, includes the remainder of the xyloglucan and much of the galacturonan. The third group, with $T_2 > 100$ ms, comprises methyl-esterified galacturonans and pectic β-(1,4′)-D-galactan. We have shown (Ha et al., 1996) that larger quantities of the polysaccharides allocated to this third group fail altogether to appear in the CP-MAS spectrum because they are particularly mobile and require much longer contact times for CP: the proton T_2 of this fraction was a few hundred microseconds (Ha et al., 1996).

Proton $T_{1\rho}$ Measurements

As in the T_2 relaxation experiment, the proton $T_{1\rho}$ values became much more widely separated after hydration as the efficiency of spin diffusion decreased, particularly in the pectic fraction of the cell wall, where spin diffusion was slowest (long proton T_2). Most resonances showed multicomponent $T_{1\rho}$ relaxation and their decay was modeled as the sum of two components, as for the T_2. The $T_{1\rho}$ relaxation curve for C-4 in the main chain of xyloglucan (Fig. 4) showed one component relaxing at a rate similar to that of cellulose, which was therefore derived from xyloglucan chains spatially associated (within about 2 nm) with the cellulose chains. The other component accounted for about one-third of the total and relaxed much faster, at a rate comparable to that of some of the pectins. The proportion of the galacturonan showing relaxation characteristics similar to cellulose was greater than in the T_2 experiment, because the longer duration of spin diffusion in the $T_{1\rho}$ experiment allowed the influence of the cellulose to be felt farther from its surface.

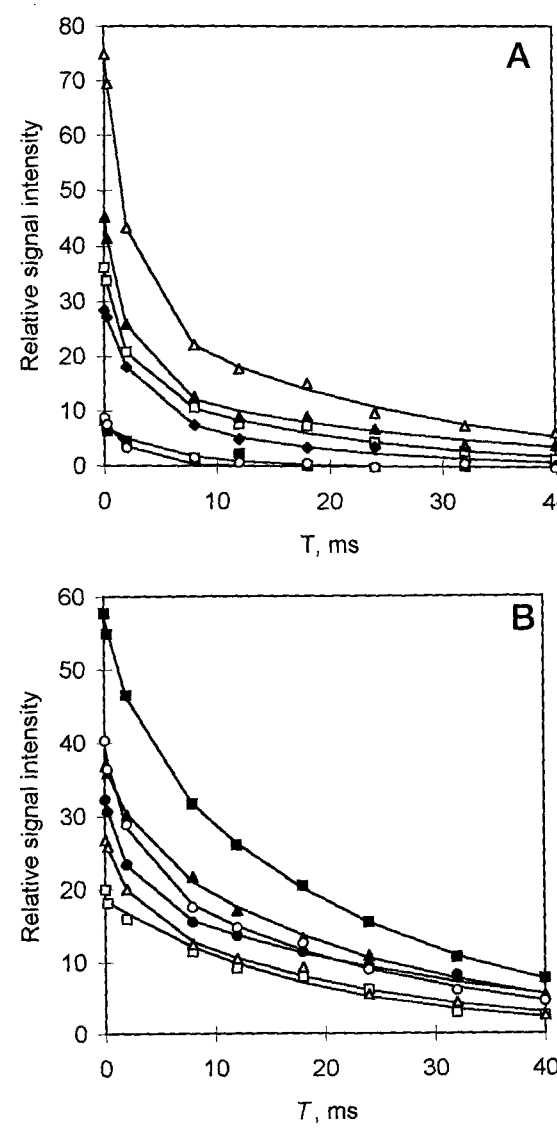

Figure 4. Proton rotating-frame $T_{1\rho}$ curves for principal peaks in the ^{13}C-NMR spectrum of hydrated onion cell walls. Rapid relaxation (short $T_{1\rho}$) implies high molecular mobility. Fitted curves are the sum of two exponential functions. A, Pectins: ■, galacturonan C-6, 171 ppm, $T_{1\rho}$ = 5.5 ms; □, galacturonan C-1, 101 ppm, $T_{1\rho}$ = 1.7 ms (57%), 19 ms (43%); ▲, galacturonan C-4, 80 ppm, $T_{1\rho}$ = 2.1 ms (66%), 28 ms (34%); △, galacturonan C-2/3, 69 ppm, $T_{1\rho}$ = 1.9 ms (60%), 24 ms (40%); ♦, pectin methoxyl, 54 ppm, $T_{1\rho}$ = 2.7 ms (63%), 16 ms (37%); and ○, acetyl, 21 ppm, $T_{1\rho}$ = 2.4 ms. B, Microfibrils: ■, cellulose/galactan C-1, 105 ppm, $T_{1\rho}$ = 2.4 ms (22%), 23 ms (78%); □, cellulose I C-4, 89 ppm, $T_{1\rho}$ = 19 ms; ▲, cellulose C-4, 84 ppm, $T_{1\rho}$ = 2.7 ms (22%), 24 ms (78%); △, xyloglucan C-4, 82.5 ppm, $T_{1\rho}$ = 2.0 ms (32%), 22 ms (68%); ●, cellulose I C-6, 65 ppm, $T_{1\rho}$ = 2.0 ms (38%), 32 ms (62%); and ○, cellulose/galactan C-6, 62 ppm, $T_{1\rho}$ = 2.1 ms (38%), 24 ms (62%).

The T_2 and $T_{1\rho}$ experiments demonstrated that cellulose and the majority of the xyloglucan formed a single solid phase in the hydrated cell walls. This phase may be assumed to correspond to the microfibrils. The remaining xyloglucan and the majority of the pectins formed a less-rigid, hydrated matrix between the microfibrils.

DISCUSSION

Cell Wall Architecture

The traditional view of the structure of the cell wall is that cellulose fibers are embedded in a matrix of other polysaccharides. The data presented here contradict this view. In hydrated onion cell walls most of the xyloglucan shared the rigidity, although not necessarily the crystallinity, of the cellulose and, therefore, the solid microfibril phase contains both of these polymers. The clearest physical distinction within the onion cell wall was between the rigid, solid cellulose/xyloglucan microfibrils and the predominantly pectic gel constituting the matrix.

A more detailed picture can be obtained by considering these NMR data in the light of the ultrastructure of the hydrated onion cell wall, which is better understood than the cell walls of any other plant (McCann et al., 1990, 1992). Three to four layers of 8- to 10-nm microfibrils, oriented approximately parallel within each layer at approximately 20-nm spacing, are stacked on one another to make up the thickness of the cell wall. The microfibrils are cross-linked by what appear to be single-polymer chains. It has been widely assumed, although on insecure evidence, that these are xyloglucans (Fry, 1986; McCann et al., 1990). The NMR data presented here and by Foster et al. (1996) support this model, since it seems reasonable to assume that the 8- to 10-nm microfibril diameter includes the rigid, adsorbed, or embedded segments of the xyloglucan chains, and to equate the cross-linking chain segments with the mobile xyloglucan fraction. This need not, of course, be applicable to all plant tissues. The cell walls in growing regions of pea hypocotyls contain more xyloglucan than onion cell walls and its extractability suggests that some of it is not closely associated with cellulose (Hayashi et al., 1987).

A new feature that can be deduced from the NMR evidence is that the pectic matrix is not homogeneous but contains "hard" and "soft" regions, on a scale of at least a few nanometers. Due to uncertainties about the rate and direction of spin diffusion, it is not possible to be more precise about the dimensions of the hard and soft regions, but they are too large to correspond to the junction zones and interjunction segments of a uniform gel.

The spectral properties of the hard regions correspond to the cable model for Ca-pectate gels (Jarvis and Apperley, 1995; Goldberg et al., 1996), with the addition of the single-chain components and some methyl-esterified aggregates (Ha et al., 1996). The pectic polysaccharides of the soft regions, the single-chain methyl-esterified galacturonans, and galactans described by Ha et al. (1996) and Foster et al. (1996) showed almost as much thermal motion as polymers in solution. We have no evidence of how the pattern of hard and soft regions in the matrix might be related to the disposition of the microfibrils in space, except that the scale seems similar. The fact that a few pectic chains were in close proximity to the microfibril surface does not necessarily imply a molecular connection to the microfibrils. It is not yet clear whether those pectic polymers that cannot readily be extracted from the cell wall are covalently bonded to the microfibrils, held by interpenetration of the two cross-linked networks, or have low intrinsic solubility.

If the hydrated onion cell wall behaves in a way similar to that of the walls of *Apium graveolens* collenchyma (Jarvis, 1992) and *Nitella opaca* cells (Probine and Preston, 1961), it can be added that each cross-linked microfibril layer provides rigidity and strength in directions parallel to the cell surface, whereas the pectic gel controls the mechanical properties of the wall across its thickness. This would imply that the xyloglucan chains cross-link microfibrils within each layer, but not between layers. In view of the NMR evidence that hydration mainly affects the pectic matrix, it would also imply that dehydration of the cell wall will collapse the interlayer spacing so that microfibrils from adjacent layers can come close to, or even touch, one another, as the wall shrinks in thickness.

Implications for the Mechanical Properties of the Cell Wall

The wide difference in rigidity between the hydrated pectins and the microfibrils, which was eliminated on dehydration, has implications for our understanding of the mechanical properties of the cell wall. Here we consider only the physical distortion of the cell wall structure by external stresses, not the enzymically mediated phenomenon of growth.

In the dry cell walls the proton-relaxation characteristics of the pectic matrix were those of a glass and the theory of composite materials can be used straightforwardly (Preston, 1979). Therefore, the rigidity of the wall depends directly on the rigidity of both the dry pectic matrix and the microfibrils, their relative contributions being derivable from a combination of the parallel (Voigt) and series (Reuss) estimates (Harris, 1980). Because of the inextensibility of the microfibrils most of the load is carried by whichever microfibrils run approximately parallel to the stress, typically within about 15° of the stress axis (Harris, 1980). On this basis a cell wall with six microfibril layers having different orientations ($90°/15° = 6$) would have stresses in any direction around the cell supported by the microfibrils. However, the onion cell wall appears to have fewer than six layers (McCann et al., 1990), so the glassy pectic matrix must carry part of the stresses within and between layers. The xyloglucan bridges probably constitute too little of the volume fraction of the matrix to have much effect, especially if they are slackened by the contraction of pectins upon drying.

In the fracture properties that control its strength, the dry cell wall may be compared with synthetic composites having a brittle matrix, e.g. glass-fiber epoxy. In such materials the matrix protects the strength of the fibers, because a fracture starting in one fiber is diverted along the matrix rather than propagating across the next fiber (Harris, 1980). Fiber-matrix adhesion is not a factor limiting strength when the fibers have such a high ratio of length to diameter ($\gg 10^2$; McCann et al., 1990).

In the hydrated cell walls, however, stresses in different directions are carried in completely different ways. There is evidence that stresses across the thickness of the cell wall are carried by pectins (Jarvis, 1992; and see above). Stresses

parallel to the microfibrils in any layer must be borne by cellulose, since it is so much less extensible than anything else in the wall. The xyloglucan bridges between microfibrils may resist stresses perpendicular to these, but we know nothing of how the cellulose-xyloglucan network constituting one layer of the wall distorts as the microfibrils are pulled apart, even in the simplest case when the external stress is of short duration and no enzymic reactions (such as those involved in growth) are involved. The xyloglucan chains may be stripped from the microfibril (Levy et al., 1991; Finkenstadt et al., 1995; Vincken et al., 1995) or pulled straight to provide "rubber" elasticity (Dorrington and McCrum, 1977), or the microfibrils may bend to give a trellis-like pattern (Boyd and Foster, 1975). The architectural complexity of the system is such that it may be appropriate to consider the hydrated cell wall as a nanostructure rather than as a composite material. If that is the case, existing materials science may give some broad guidelines as to its mechanical behavior, but a more detailed picture will need to be worked out from first principles.

ACKNOWLEDGMENTS

The authors thank Drs. B.W. Evans, M.J. Gidley, R. Newman, and J.F.V. Vincent for advice.

Received January 13, 1997; accepted June 30, 1997.

LITERATURE CITED

Abragam A (1961) Principles of Nuclear Magnetism. Clarendon Press, Oxford, UK

Boyd JD, Foster RC (1975) Microfibrils in primary and secondary wall growth develop trellis configurations. Can J Bot **53:** 2687–2701

Dorrington KL, McCrum NG (1977) Elastin as a rubber. Biopolymers **16:** 1201–1222

Finkenstadt VL, Hendrixson TL, Millane RP (1995) Models of xyloglucan binding to cellulose microfibrils. J Carbohydr Chem **14:** 601–611

Foster TJ, Ablett S, McCann MC, Gidley MJ (1996) Mobility-resolved C-13-NMR spectroscopy of primary plant-cell walls. Biopolymers **39:** 51–66

Fry SC (1986) Cross-linking of matrix polymers in the growing cell-walls of angiosperms. Annu Rev Plant Physiol **37:** 165–186

Goldberg R, Morvan C, Jauneau A, Jarvis MC (1996) Methyl-esterification, de-esterification and gelation of pectins in the primary cell wall. *In* J Visser, AGJ Voragen, eds, Pectins and Pectinases. Elsevier, Amsterdam, pp 151-172

Ha MA, Evans BW, Jarvis MC, Apperley DC, Kenwright AM (1996) CP-MAS NMR of highly mobile hydrated biopolymers: polysaccharides of *Allium* cell walls. Carbohydr Res **288:** 15–23

Harris B (1980) Composite materials. *In* JFV Vincent, JD Currey, eds, The Mechanical Properties of Biological Materials. Cambridge University Press, Cambridge, UK, pp 37–74

Hayashi T, Marsden MPF, Delmer DP (1987) Pea xyloglucan and cellulose. VI. Xyloglucan-cellulose interactions *in vitro* and *in vivo*. Plant Physiol **83:** 384–389

Irwin PL, Gerasimowicz WV, Pfeffer PE, Fishman M (1985) H-1-C-13 polarization transfer studies of uronic-acid polymer systems. J Agric Food Chem **33:** 1197–1201

Irwin PL, Pfeffer PE, Gerasimowicz WV, Pressey R, Sams CE (1984) Ripening-related perturbations in apple cell-wall nuclear-spin dynamics. Phytochemistry **23:** 2239–2242

Ishii S (1982) Enzymic extraction and linkage analysis of pectic polysaccharides from onion. Phytochemistry **21:** 778–780

Jarvis MC (1990) Solid state ^{13}C-n.m.r. spectra of *Vigna* primary cell walls and their polysaccharide components. Carbohydr Res **201:** 327–333

Jarvis MC (1992) Control of thickness of collenchyma cell walls by pectins. Planta **187:** 218–220

Jarvis MC, Apperley DC (1995) Chain conformation in concentrated pectic gels: evidence from ^{13}C NMR. Carbohydr Res **275:** 131–145

Jarvis MC, Fenwick KM, Apperley DC (1996) Cross-polarisation kinetics and proton NMR relaxation in polymers of *Citrus* cell walls. Carbohydr Res **288:** 1–14

Kenwright AM, Say BJ (1993) Solid-state NMR studies of polymers. *In* RN Ibbett, ed, NMR Spectroscopy of Polymers. Blackie, London, pp 232–274

Levy S, York WS, Stuikeprill R, Meyer B, Staehelin LA (1991) Simulations of the static and dynamic molecular-conformations of xyloglucan: the role of the fucosylated side-chain in surface-specific side-chain folding. Plant J **1:** 195–215

McBrierty VJ, Packer KJ (1994) NMR in Solid Polymers. Cambridge University Press, Cambridge, UK

McCann MC, Wells B, Roberts K (1990) Direct visualization of cross-links in the primary plant-cell wall. J Cell Sci **96:** 323–334

McCann MC, Wells B, Roberts K (1992) Complexity in the spatial localization and length distribution of plant cell-wall matrix polysaccharides. J Microsc **166:** 123–136

Mankarios AT, Hall Ma, Jarvis MC, Threlfall DR, Friend J (1979) Cell wall polysaccharides from onions. Phytochemistry **19:** 1731–1733

Newman RH (1992) Nuclear magnetic resonance study of spatial relationships between chemical components in wood cell walls. Holzforschung **46:** 205–210

Newman RH, Davies LM, Harris PJ (1996) Solid-state ^{13}C nuclear magnetic resonance characterization of cellulose in the cell walls of *Arabidopsis thaliana* leaves. Plant Physiol **111:** 475–485

Newman RH, Ha MA, Melton LD (1994) Molecular ordering of cellulose in apple cell walls. J Agric Food Chem **42:** 1402–1406

Preston RD (1979) Polysaccharide conformation and cell wall function. Annu Rev Plant Physiol **30:** 55–78

Probine MC, Preston RD (1961) Cell growth and the structure and mechanical properties of the wall in internodal cells of *Nitella opaca*. I. Wall structure and growth. J Exp Bot **12:** 261–282

Raven JA (1977) The evolution of vascular land plants in relation to supracellular transport processes. Adv Bot Res **5:** 153–219

Redgwell RJ, Selvendran RR (1986) Structural features of cell-wall polysaccharides of onion *Allium cepa*. Carbohydr Res **157:** 183–199

Ryden P, Colquhoun IJ, Selvendran RR (1989) Investigations of structural features of the pectic polysaccharides of onion by ^{13}C n.m.r spectroscopy. Carbohydr Res **185:** 233–237

Schaefer J, Stejskal EO, Buchdahl R (1977) Magic-angle ^{13}C NMR analysis of motion in solid glassy polymers. Macromolecules **10:** 384–405

Tekely P, Vignon MR (1987) Proton T_1 and T_2 relaxation times of wood components using ^{13}C CP/MAS NMR. J Polym Sci C Polym Lett **25:** 257–261

Vincken JP, Dekeizer A, Beldman G, Voragen AGJ (1995) Fractionation of xyloglucan fragments and their interaction with cellulose. Plant Physiol **108:** 1579–1585